Available online at www.sciencedirect.com

ScienceDirect

Energy Procedia 49 (2014) 478 – 487

Energy Procedia

SolarPACES 2013

# Optimization of high temperature SiC volumetric solar absorber

S. Mey[a]*, C. Caliot[a], G. Flamant[a], A. Kribus[b], Y. Gray[b]

[a] *PROMES–CNRS Laboratory (UPR 8521), 7 rue du Four Solaire, 66120 Font-Romeu-Odeillo-Via, France*
[b] *School of Mechanical Engineering, Tel Aviv University, Tel Aviv 69978, Israel*

**Abstract**

Focusing on radiative properties (absorption and scattering coefficient, scattering phase-function) of silicon carbide foams, several predictive models are compared to spectral transmittance and reflectance measurements (bi-directional and directional-hemispherical) in the aim of determining new correlations based on ceramic foam characteristics (struts/pores size and porosity). A mono-dimensional modeling is developed to solve Navier-stokes equations (conservation of mass and momentum) and energy equations (coupled heat transfers) inside the absorber. Several radiative models are tested to approximate the radiative transfer equation end compute the radiative source term (Rosseland, P-1 model, and two-flux approximation). Numerical simulations are compared to reference results obtained with Monte-Carlo algorithm using net-exchange formulation.



Selection and peer review by the scientific conference committee of SolarPACES 2013 under responsibility of PSE AG.
Final manuscript published as received without editorial corrections.
*Keywords: volumetric solar absorber; concentrated solar power (CSP); porous medium, reticulate porous ceramic (RPC); ceramic foam; silicon carbide (SiC); Navier-Stokes equations; flow modelling; pressure drop; Darcy-Forchheimer law; coupled heat transfers; conduction; convection; radiation; Rosseland; P-1 model; two-flux approximation; Monte-Carlo.*

## 1. Introduction

Radiative heat transfer inside porous medium is thoroughly studied in many systems such as burners, chemical catalysts, and concentrated solar power. The present article will focus on volumetric solar absorbers made of reticulated porous ceramics (RPC) made of Silicon Carbide (SiC) and modelling radiative heat transfer inside those high temperature solar absorbers.

* Corresponding author. Tel.: +33(0)4.6830.77.63
*E-mail address:* sebastien.mey@promes.cnrs.fr


Selection and peer review by the scientific conference committee of SolarPACES 2013 under responsibility of PSE AG.
Final manuscript published as received without editorial corrections.
doi:10.1016/j.egypro.2014.03.051

For a better understanding of radiative properties of ceramic foams and reticulate porous ceramics made of silicon carbide, reflectance and transmittance measurements are conducted. Identification methods are used to identify the extinction, absorption and scattering coefficients from experimental data. Then, combined heat and flow transfers are modelled with three different radiative approximations: the Rosseland conductivity model, the P-1 model, and the Two-Flux approximation. To base our numerical study on a reference case, a Monte-Carlo algorithm is used to solve the radiative equation and get reference results.

**Nomenclature**

*Latin symbols*

| | |
|---|---|
| $A$ | Aperture surface $[m^2]$ |
| $A_v$ | Specific surface $[m^2.m^{-3}]$ |
| $C_p$ | Specific heat $[J.kg^{-1}.K^{-1}]$ |
| $d_c$ | Cell diameter $[mm]$ |
| $d_p$ | Pore diameter $[mm]$ |
| $D$ | Diffusive coefficient of P–1 model $[m]$ |
| $E$ | Amount of energy $[J]$ |
| $\vec{f}$ | Volumetric force $[N.kg^{-1}]$ |
| $G$ | Total irradiation $[W.m^{-2}]$ |
| $h_v$ | Convective heat transfer coef. $[W.K^{-1}.m^{-2}]$ |
| $i$ | Luminance $[W.m^{-2}.sr^{-1}]$ |
| $i_b$ | Black-body luminance $[W.m^{-2}.sr^{-1}]$ |
| $K_1$ | Permeability coefficient $[m^2]$ |
| $K_2$ | Inertial coefficient $[m]$ |
| $k$ | Thermal conductivity $[W.m^{-1}.K^{-1}]$ |
| $k_a$ | Absorption coefficient $[m^{-1}]$ |
| $k_d$ | Scattering coefficient $[m^{-1}]$ |
| $k_R$ | Radiative conductivity $[W.m^{-1}.K^{-1}]$ |
| $\dot{m}$ | Mass flow rate $[kg.s^{-1}]$ |
| $P$ | Pressure $[Pa]$ |
| $P_{atm}$ | Atmospheric pressure $[Pa]$ |
| $\vec{Q}$ | Flux vector $[W.m^{-2}]$ |
| $q_r$ | Radiative flux $[W.m^{-2}]$ |
| $q_{r,loss}$ | Radiative losses $[W.m^{-2}]$ |
| $q_{solar}$ | Solar flux $[W.m^{-2}]$ |
| $r$ | Specific Ideal Gas constant of air |
| $S$ | Source term $[W.m^{-3}]$ |
| $s$ | Sample thickness $[mm]$ |
| $T$ | Temperature $[K]$ |
| $u$ | Fluid velocity $[m.s^{-1}]$ |
| $\vec{v}$ | Velocity vector $[m.s^{-1}]$ |

*Greek symbols*

| | |
|---|---|
| $\alpha$ | Absorptivity / absorptance $[-]$ |
| $\beta$ | Extinction coefficient $[m^{-1}]$ |
| $\varepsilon$ | Porosity $[-]$ |
| $\eta_{S2T}$ | Solar-to-thermal efficiency $[-]$ |
| $\theta$ | Direction angle $[rad]$ |
| $\lambda$ | Wavelength $[\mu m]$ |
| $\lambda_{bulk}$ | Conductivity of bulk material $[W.m^{-1}.K^{-1}]$ |
| $\mu$ | Dynamic viscosity $[Pa.s]$ |
| $\rho$ | Density $[kg.m^{-3}]$ |
| $\sigma$ | Stefan-Boltzmann constant |
| $\tau_{opt}$ | Optical thickness $[-]$ |
| $\varphi$ | Solar flux $[W.m^{-2}]$ |
| $\omega$ | Scattering albedo $[-]$ |

*Composed symbols*

| | |
|---|---|
| $HDR$ | Hemispherical-directional reflectance $[-]$ |
| $HDT$ | Hemispherical-directional transmittance $[-]$ |
| $Nu$ | Nusselt number $[-]$ |
| $Re$ | Reynolds number $[-]$ |
| $\Delta H_f$ | Out-in fluid enthalpy difference $[J.kg^{-1}]$ |

*Superscripts and subscripts*

| | |
|---|---|
| $X^{(0)}$ | Zeroth moment of P-N development |
| $X^{(1)}$ | First moment of P-N development |
| $X^{(+)}$ | Forward direction |
| $X^{(-)}$ | Backward direction |
| $X^*$ | Effective physical quantity |
| $X_f$ | Relative to fluid |
| $X_{in}$ | Relative to inlet |
| $X_{out}$ | Relative to outlet |
| $X_s$ | Relative to solid |
| $X_\lambda$ | Spectral physical quantity |

## 2. Radiative properties of SiC foams

Several works have already been done to obtain radiative properties of RPCs, and we may identify three major ways: 1- identification based on transmittance and reflectance measurements [1,2,3,4]; 2- the Ray Tracing Method (RTM) inside 3D reconstructed geometry (3D numerical foams) [2,3,5]; 3- a geometrical optics approach based on idealized foam structures [6,7,8].

The first method has been used on different levels depending on how detailed you need to get the radiative properties : for instance, extinction coefficient is obtained from transmittance measurements; absorption and

scattering coefficients are obtained from transmittance and reflectance measurements; the scattering phase function is obtained from such directional measurements.

The second method is quite new compared to the two others and involve Monte-Carlo ray tracing algorithms to be able to compute the radiative properties. It requires a numerical 3D foam structure with surface condition.

The final method is more complex to use, because of the difficulties to obtain the struts dimensions of ceramic foam. They are considered as the scatterers and absorbers inside the porous medium and correlations are based on their geometrical characteristics (length, thickness, geometry and orientation).

Here, we will obtain radiative properties of SiC foams using an identification model based on transmittance and reflectance measurements.

### *2.1. Experimental radiative properties identification*

Measurements were conducted at the PROMES Laboratory using a directional-hemispherical reflectometer (SOC100-HDR from Surface Optics Corporation) made of an elliptic reflective dome (two focal points). At the moment, spectral measurements were done in the wavelength range $2-15\mu m$ (infrared). Results were obtained for two types of measurements: Hemispherical-Directional Reflectance (HDR) and Hemispherical-Directional Transmittance (HDT).

The absorptance was obtained as in Eq.1: it is a "volumetric" absorptance, taking into account the scattered then absorbed rays inside the sample.

$$\alpha_\lambda = 1 - HDR_\lambda - HDT_\lambda \tag{1}$$

Different pore size and porosity were tested, for samples (25×25 mm) with various thicknesses (see table 1).

Table 1. Sic foam samples characteristics.

| Sample number | Sample #1 | Sample #2 | Sample #3 | Sample #4 | Sample #5 |
|---|---|---|---|---|---|
| Porosity | 0.748 | 0.722 | 0.796 | 0.762 | 0.823 |
| Pore diameter $[mm]$ | 1.03 | 0.933 | 1.25 | 1.32 | 1.07 |
| Thicknesses $[mm]$ | 2.58 (a)<br>3.44 (b) | 1.86 (a)<br>3.17 (b) | 2.02 (a)<br>2.95 (b) | 1.65 (a)<br>2.63 (b) | 2.93 |

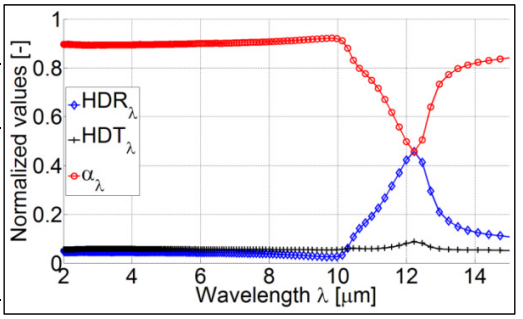


Figure 1. Spectral HDR and HDT measurements and volumetric absorptance for sample #1a.

### *2.2. Identification method*

As a first approach, identification was made using Bouguer's law (also called Beer-Lambert's law), assuming proportional dependence between sample thickness and HDT logarithm (Eq.2):

$$\beta_\lambda = \frac{-ln(HDT_\lambda)}{s} \tag{2}$$

In a second time, to make distinction between absorption and scattering coefficients the Fresnel number $F = a^2/(\lambda r)$ is used to determine whether diffraction occurs inside RPCs ($a$ is the distance between the diffracter and the screen (here, the distance between two struts corresponding to the mean cell size), $\lambda$ is the wavelength of the incident radiation and $r$ is the dimension of the diffracter (here, the struts)). For the studied RPCs, typical values are

$a = 1mm$ (mean cell size) and $r = 0.2mm$ (struts diameter), which lead to Fresnel numbers in the range $333 - 2500$. As this value is larger than unity, we may neglect diffraction and scattering is only due to reflection.

It finally assumes the scattering albedo to be equal to the sum of HDR and HDT ($\omega_\lambda = HDR_\lambda + HDT_\lambda$). Thus, absorption and scattering coefficients are obtained as in Eq.3:

$$\begin{cases} k_a = \alpha_\lambda \beta_\lambda \\ k_d = (1 - \alpha_\lambda)\beta_\lambda \end{cases} \quad (3)$$

## 3. Modeling of solar volumetric absorber

### *3.1. Equation model*

#### *3.1.1. Assumptions*

The 1D model of combined flow and heat transfer in the porous absorber is based o several assumptions: a) The fluid (air) is an Ideal Gas; b) Because of the large temperature variation of the fluid, its thermal properties are considered temperature dependent; c) Because of the lower temperature variation of the solid phase, its thermal properties are considered constant; d) The solid phase (SiC) is supposed radiatively grey; e) The incident solar power is perfectly diffuse and uniform; f) The flow is supposed laminar inside the porous medium; g) The effective medium characteristics are supposed uniform (porosity and pore diameter); h) The steady state is established; i) The heat due to viscous effects and volume compression is neglected; j) No volumetric forces (gravity) are applied to the fluid; k) Wall effects are neglected inside the absorber (1D geometry).

#### *3.1.2. Flow equations*

The 1D continuity equation allows us to obtain the fluid velocity from the mass flow rate:

$$d_x(\rho u) = 0 \ \rightarrow \ u = \frac{\dot{m}}{\rho A} \quad (4)$$

The 1D momentum equation is given by:

$$d_x\left(\frac{\rho u u}{\varepsilon}\right) = -\varepsilon d_x P - \varepsilon u\left(\frac{\mu}{K_1} + \frac{\rho}{K_2} u\right) \quad (5)$$

Combining Eq.4 and Eq.5 allows us to transform the momentum equation into a pressure equation:

$$-d_x P = \left(\frac{\dot{m}}{A\varepsilon}\right)^2 d_x\left(\frac{1}{\rho}\right) + \frac{\mu}{K_1}\frac{\dot{m}}{\rho A} + \frac{\rho}{K_2}\left(\frac{\dot{m}}{\rho A}\right)^2 \quad (6)$$

#### *3.1.3. Energy equations*

The local thermal non-equilibrium model is used to obtain separately the fluid temperature and the solid structure temperature (named after solid temperature). Thus, the energy equation for the fluid phase is:

$$d_x\left(\rho C_p T_f u\right) = d_x\left(k_f d_x T_f\right) + h_v\left(T_s - T_f\right) \quad (7)$$

And the energy equation for the solid phase is:

$$0 = d_x(k_s^* d_x T_s) + h_v\left(T_f - T_s\right) - d_x q_r \quad (8)$$

The radiative source term $(-d_x q_r)$ (divergence of radiative flux) is computed using different radiative models.

*3.1.4. Radiative models*

Several approximations exist to solve the radiative transfer equation in different medium. Concerning porous medium, the same assumption is commonly supposed: equivalent homogeneous medium. So far, different models could be used to model radiative heat transfer inside porous medium used as volumetric solar receiver: the Rosseland conductivity [9,10], the P-1 model [11,12], the two-flux approximation [13], and Monte-Carlo [14].

The work in here is to compare these models in the case of a solar absorber made of silicon carbide ceramic foam. So, as said in the introduction, three radiative models are tested and compared to Monte-Carlo results (reference results).

*3.1.4.1. Rosseland conductivity model*

This radiative approximation is the simplest to be accounted for. It is used for optically thick media, where optical thickness is much greater than unity ($\tau_{opt} \gg 1$).

So far, we know than the Rosseland conductivity model is not adapted for solar power modeling, because errors are large near boundaries. However, we still have tested it in the aim of proving or invalidating its use in the case of volumetric solar absorber.

The Rosseland approximation assumes radiation inside the medium to behave as thermal diffusion. Thus, the radiative flux is only affected by close neighbors and is written as follow [15]:

$$q_r = -\frac{16\sigma}{3\beta} T_s^3 d_x T_s = -k_R d_x T_s \tag{9}$$

Finally, its implementation is realized by modifying the conduction term in the energy equation for the solid phase:

$$0 = d_x[(k_s^* + k_R) d_x T_s] + h_v\left(T_f - T_s\right) \tag{10}$$

*3.1.4.2. P–1 model*

This radiative model comes from the general P–N method, involving spherical harmonics series – also called the moment method. For the P–1 model, the major hypothesis assumes isotropic radiation inside the medium (see Fig. 2). Its development leads to consider the zeroth and first spherical harmonics [16]:

$$i = \frac{1}{4\pi}\left[i^{(0)} + 3\cos\theta\, i^{(1)}\right] = \frac{1}{4\pi}[G + 3\cos\theta\, q_r] \tag{11}$$

As detailed in [16], the closure condition for the P-1 model allows us to find a relation between the zeroth ($i^{(0)} = G$) and the first ($i^{(1)} = q_r$) spherical harmonics:

$$\begin{cases} d_x q_r = k_a(4\pi i_b - G) \\ \frac{1}{3\beta} d_x G = -q_r \end{cases} \tag{12}$$

Combining Eq.12 leads to a diffusion equation with source term to obtain the total irradiation G.

$$-d_x(D d_x G) = k_a(4\sigma T_s^4 - G) \tag{13}$$

Once we have the total irradiation from Eq.13, we are able to compute the radiative source term using first Eq.12.

*3.1.4.3. Two-flux approximation*

This approximation is a specific case of a more general method called the discrete ordinates method. In here, the 4π steradians are discretised and radiative transfer equation is solved along the optical path for each discretized solid angle (i.e. for each direction).

Concerning the two-flux approximation, the directions are separated into two hemispheres noted $(+)$ for the forward direction and $(-)$ for the backward direction. Thus, we have a set of two equations, respectively for the forward luminance $i^{(+)}$ and the backward luminance $i^{(-)}$ [17], assuming that they are isotropic over each hemisphere (see Fig.1):

$$\begin{cases} \frac{1}{2\beta} d_x i^{(+)} = (1-\omega) i_b - i^{(+)} + \frac{\omega}{2}\left[i^{(+)} + i^{(-)}\right] \\ -\frac{1}{2\beta} d_x i^{(-)} = (1-\omega) i_b - i^{(-)} + \frac{\omega}{2}\left[i^{(+)} + i^{(-)}\right] \end{cases} \quad (14)$$

Several relations may be obtained from these assumptions, and before solving the equations:

- The total luminance is obtained by summing the forward and backward contributions;
- The total irradiation is obtained by integrating luminance over all directions;
- The radiative flux is obtained by integrating luminance times $\cos\theta$ over all directions.

$$\begin{cases} i = i^{(+)} + i^{(-)} \\ G = 2\pi\left[i^{(+)} + i^{(-)}\right] \\ q_r = \pi\left[i^{(+)} - i^{(-)}\right] \end{cases} \quad (15)$$

And finally, the radiative source term is computed the same way than Eq.12:

$$-d_x q_r = k_a\left\{4\sigma T_s^4 - 2\pi\left[i^{(+)} + i^{(-)}\right]\right\} \quad (16)$$

The implementation is then realized the same way as for the previous radiative model:

$$0 = d_x(k_s^* d_x T_s) + h_v\left(T_f - T_s\right) - k_a\left\{4\sigma T_s^4 - 2\pi\left[i^{(+)} + i^{(-)}\right]\right\} \quad (17)$$

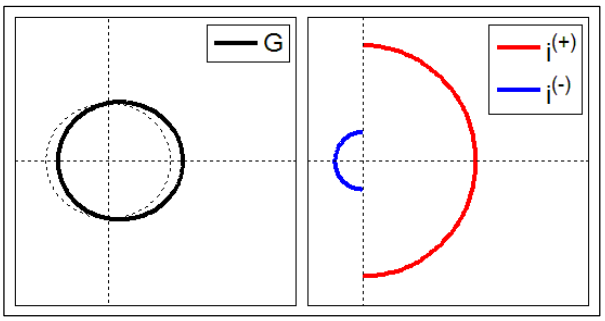


Figure 2. Qualitative luminances form of P–1 model (left) and Two-Flux approximation (right).

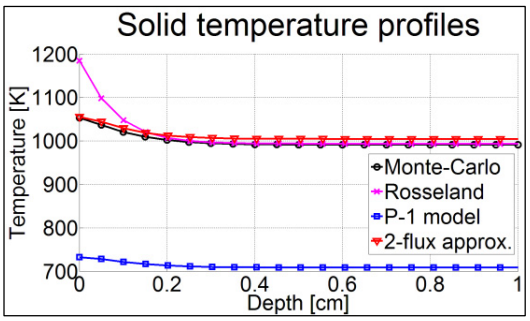


Figure 3. Solid temperature profiles inside the absorber after convergence.

*3.1.5. Boundary conditions*

Here, we assume a volumetric medium with no physical front surface. This leads to the following boundary condition treatments depending on the radiative approximation used in the modeling.

*3.1.5.1. Navier-Stokes boundary conditions*

The modeled absorber is an atmospheric air absorber. So far, the pressure boundary condition is the outlet pressure, fixed as the atmospheric pressure to match the future experimental conditions for model validation:

$$P_{out} = P_{atm} \tag{18}$$

*3.1.5.2. Energy boundary conditions*

The inlet temperatures boundary conditions are as follow:

$$\begin{cases} T_{f,in} = T_{amb} \\ d_x T_s|_{in} = 0 \end{cases} \tag{19}$$

We also suppose thermal equilibrium with environment at outlet, leading to:

$$\begin{cases} d_x T_f\big|_{out} = 0 \\ d_x T_s|_{out} = 0 \end{cases} \tag{20}$$

*3.1.5.3. Radiative boundary conditions*

For all radiative models, the form of the boundary condition is the following:

$$\begin{cases} q_{r,in} = q_{solar,in} - q_{r,loss} = \varphi - q_{r,loss} \\ q_{r,out} = 0 \end{cases} \tag{21}$$

Thus, every radiative model has its specific formulation of this boundary condition:

- Rosseland conductivity model – here, we take into account the emission losses from the inlet of the volumetric medium without reflection and back-scattering, as radiation is totally absorbed and then behaves as conduction (this boundary condition replaces the solid temperature boundary condition previously exposed);

$$\begin{cases} -k_R d_x T_s|_{in} = \varphi - \alpha\sigma(T_s^4 - T_{amb}^4) \\ -k_R d_x T_s|_{out} = 0 \end{cases} \tag{22}$$

- P-1 model – the radiative losses come from the luminance form (quasi-isotropic), considering half of inlet total irradiation;

$$\begin{cases} -\frac{1}{3\beta} d_x G|_{in} = \varphi - \frac{G_{in}}{2} \\ -\frac{1}{3\beta} d_x G|_{out} = 0 \end{cases} \tag{23}$$

- Two-flux approximation – the set of two equations depending on the direction allow us to separate the solar component of the luminance ($i_{in}^{(+)}$), and the radiative losses ($i_{in}^{(-)}$) obtained after convergence;

$$\begin{cases} i_{in}^{(+)} = \frac{\varphi}{\pi} \\ i_{out}^{(-)} = \frac{\sigma T_s^4}{\pi} \end{cases} \tag{24}$$

### 3.2. Properties models

#### 3.2.1. Fluid thermal properties

The fluid density is given by the Ideal Gas law:

$$\rho = \frac{P}{rT_f} \tag{25}$$

The specific heat $C_p$, the dynamic viscosity μ and the thermal conductivity $k_f$ are temperature dependent polynomial relations:

$$\begin{cases} C_p = 1060 + 0{,}449T_f + 1{,}14 \cdot 10^{-3}T_f^2 - 8 \cdot 10^{-7}T_f^3 + 1{,}93 \cdot 10^{-10}T_f^4 \\ \mu = 1{,}13 \cdot 10^{-6} + 7{,}06 \cdot 10^{-8}T_f - 4{,}87 \cdot 10^{-11}T_f^2 + 2{,}66 \cdot 10^{-14}T_f^3 - 6{,}12 \cdot 10^{-18}T_f^4 \\ k_f = -3{,}94 \cdot 10^{-4} + 1{,}02 \cdot 10^{-4}T_f - 4{,}86 \cdot 10^{-8}T_f^2 + 1{,}52 \cdot 10^{-11}T_f^3 \end{cases} \tag{26}$$

#### 3.2.2. Solid thermal properties

The effective thermal conductivity of the solid phase was obtained from [18]:

$$k_s^* = \frac{(1-\varepsilon)}{3}\lambda_{bulk} \tag{27}$$

#### 3.2.3. Pressure drop coefficients

The pressure equation given by the momentum equation takes into account the pressure drop due to the porous medium, involving the viscous permeability $K_1$ and the inertial permeability $K_2$. Those two parameters were numerically obtained conducting simulation on ideal tetrakaidecahedron-mesh foam structure, and experimentally validated at ambient temperature [19]. We suppose its validity at high fluid temperature.

$$\begin{cases} K_1 = \frac{{d_c}^2}{1039-1002\varepsilon} \\ K_2 = \frac{d_c}{0{,}538\varepsilon^{-5{,}739}} \end{cases} \tag{28}$$

#### 3.2.4. Convective heat exchange

Using adimensional correlations based on volumetric Nusselt number and Reynolds number, the convective heat transfer coefficient was numerically obtained from simulation [20].

$$\begin{cases} Nu_v = \frac{h_v d_c}{k_f} \\ Re = \frac{\rho u d_c}{\mu} \\ Nu_v = 2{,}0696A_v Re^{0{,}438} \end{cases} \tag{29}$$

Involving ideal tetrakaidecahedron-mesh foam structure, the specific surface area was calculated from the following relation:

$$A_v = \frac{-8{,}278\varepsilon^{0{,}38} + 57{,}384\varepsilon^{1{,}38} - 106{,}63\varepsilon^{2{,}38} + 95{,}756\varepsilon^{3{,}38} - 37{,}24\varepsilon^{4{,}38}}{d_c} \tag{30}$$

*3.2.5. Radiative properties*

As a first approach, the radiative properties were computed using Hendricks & Howell model [1]. Thus, two relations allow us to obtain the absorption coefficient and the scattering coefficient (supposing isotropic scattering phase-function).

$$\begin{cases} k_a = 4.8\alpha\frac{(1-\varepsilon)}{d_p} \\ k_d = 4.8(1-\alpha)\frac{(1-\varepsilon)}{d_p} \end{cases} \quad (31)$$

## 4. Numerical comparison

Post-processing of results lead to compute the fluid enthalpy and the solar-to-thermal efficiency as follow:

$$\eta_{s2t} = \frac{\dot{m}\Delta H_f}{\varphi A} = \frac{\dot{m}\int_{T_{f,in}}^{T_{f,out}} C_p dT}{\varphi A} \quad (32)$$

In the aim of finding the best radiative model to compute the radiative source term for 1D modeling of volumetric solar air receiver, we will compare temperature fields for the three presented radiative models to Monte-Carlo results (see table 4).

Table 2. Simulation results after convergence for all radiative models.

| Model | Rosseland | P–1 model | Two-flux approximation | Monte-Carlo |
|---|---|---|---|---|
| Calculation time | 0.76 $s$ | 1.39 $s$ | 0.93 $s$ | $\sim 2.51\ h$ |
| Energy residual | 0 % | $-7.68\cdot10^{-4}$ % | $-1.84\cdot10^{-3}$ % | |
| Inlet solid temperature | 1183 $K$ | 747 $K$ | 1073 $K$ | 1054 $K$ |
| Outlet fluid temperature | 991 $K$ | 706 $K$ | 1002 $K$ | 991 $K$ |
| Pressure drop | $-665\ Pa$ | $-405\ Pa$ | $-671\ Pa$ | $-660\ Pa$ |
| Solar-to-thermal efficiency | 87.56 % | 49.91 % | 88.93 % | 87.57 % |

After convergence of all simulations, temperature profiles were obtained (see Fig.3).

Due to the specific form of the luminance for the P–1 model (see Fig.1), radiative losses are overestimated leading to a lower fluid temperature ($-280$ K compared to Monte-Carlo).

As expected, the Rosseland conductivity is not accurate near the boundary (higher inlet solid temperature), but is accurate inside the absorber ($\overline{\Delta T_s} < 0.5$K).

Concerning the two-flux approximation, solid temperature profile is very close to the Monte-Carlo results, with average temperature difference about 13 K.

## 5. Conclusion

First measurements were obtained for several foam samples (different porosity and pore diameter) with various thicknesses. The Bouguer's law was used as a first approach to obtain the spectral radiative coefficients.

The future steps are to conduct spectral measurements in the visible and near-IR wavelength range, and to use other identification methods (such as Monte-Carlo to obtain the phase-function).

Based on the comparison of different radiative heat transfers models, the two-flux approximation should be used when optimization algorithms will be implemented in the 1D geometry. An experimental validation of the model is still needed, and will be done as soon as possible.

## Acknowledgements

The authors are very thankful to the OPTISOL project from the ANR France (National Agency for Research, program SEED 2011, project ref. ANR-11-SEED-0009).

The authors also thank the support from the Ministry of Foreign Affairs (France), the Ministry of National Education and Research (France), and the Ministry of Science and Technology (Israel).

## References

[1] Hendricks TJ, Howell JR. Absorption/scattering coefficients and scattering phase functions in reticulated porous ceramics. ASME Journal of Heat Transfer 1996; 118:79–87.
[2] Petrasch J, Wyss P, Steinfeld A. Tomography-based Monte-Carlo determination of radiative properties of reticulate porous ceramics. Journal of Quantitative Spectroscopy & Radiative Transfer 2007; 105:180–197.
[3] Partharasaty P, Habisreuther P, Zarzalis N. Identification of radiative properties of reticulated ceramic porous inert media using ray tracing technique. Journal of Quantitative Spectroscopy & Radiative Transfer 2012; 113:1961–1969.
[4] Celzard A, Tondi G, Lacroix D, Jeandel G, Monod B, Fierro V, Pizzi A. Radiative properties of tannin-based, glasslike, carbon foams. Carbon 2012; 50:4102–4113.
[5] Akolkar A, Petrasch J. Tomography based pore-level optimization of radiative transfer in porous media. International Journal of Heat and Mass Transfer 2011; 54:4775–4783.
[6] Torpey MR. A study of radiative heat transfer trough foam insulation. Master's thesis, Massachusetts Institute Of Technology, 1987.
[7] Baillis D, Raynaud M, Sacadura J. Spectral radiative properties of open-cell foam insulation. Journal of Thermophysics and Heat Transfer 1999; 13:292–298.
[8] Baillis D, Raynaud M, Sacadura J. Determination of spectral radiative properties of open cell foam: Model validation. Journal of Thermophysics and Heat Transfer 2000; 14:137–143.
[9] Smirnova O, Fend T, Scharwzbozl P, Schollgen D. Homogeneous and inhomogeneous model for flow and heat transfer in porous materials as high temperature solar air receivers. Excerpt from the Proceedings of the COMSOL Conference, Paris, France, 2010.
[10] Sano Y, Iwase S, Nakayama A. A local thermal nonequilibrium analysis of Silicon carbide ceramic foam as a solar volumetric receiver. Journal of Solar Energy Engineering 2012; 134:021006 1-8.
[11] Wu Z, Caliot C, Bai F, Flamant G, Wang Z. Coupled radiation and flow modeling ceramic foam volumetric solar air receivers. Solar Energy 2011; 85:2374–2385.
[12] Wu Z, Wang Z. Fully coupled transient modelling of ceramic foam volumetric solar air receiver. Solar Energy 2013; 89:122–133.
[13] Gomez MA, Patino D, Comesana R, Porteiro J, Alvarez Feijo MA, Miguez JL. CFD simulation of solar radiation absorber. International Journal of Heat and Mass Transfer 2013; 57:231–240.
[14] Cheng ZD; He YL, Cui FQ. Numerical investigations on coupled heat transfer and synthetical performance of pressurized volumetric receiver with MCRT-FVM method. Applied Thermal Engineering 2013; 50:1044–1054.
[15] Siegel R, Howell JR. Thermal Radiation Heat Transfer, chapter 15-3, pages 748–751. Taylor & Francis, 1992.
[16] Siegel R, Howell JR. Thermal Radiation Heat Transfer, chapter 15-5, pages 779–781. Taylor & Francis, 1992.
[17] Siegel R, Howell JR. Thermal Radiation Heat Transfer, chapter 15-6, pages 785–789. Taylor & Francis, 1992.
[18] Kamiuto K. Cellular and Porous Materials: Thermal Properties Simulation and Prediction, Modelling of composite heat transfer in open-cellular porous materials at high temperatures, chapter 6. Eds A. Öchsner, G. E. Murch and M. J. S. de Lemos, 2008.
[19] Wu Z, Caliot C, Bai F, Flamant G, Wang Z, Zhang J, Tian C. Experimental and numerical study on pressure drop in ceramic foams for volumetric solar receiver applications. Applied Energy 2010; 87:504–513.
[20] Wu Z, Caliot C, Bai F, Flamant G, Wang Z. Numerical simulation of convective heat transfer between air flow and ceramic foams to optimise volumetric solar air receivers. International Journal of Heat and Mass Transfer 2011; 54:1527–1537.